

Original Article

Influence of SiC content on the oxidation of carbon fibre reinforced ZrB₂/SiC composites at 1500 and 1650 °C in air

Antonio Vinci  , Luca Zoli , Diletta Sciti 

<https://doi.org/10.1016/j.jeurceramsoc.2018.04.064>

Highlights

- Rapid exposition to high temperature triggers the quick formation of a protective glass phase.
- The **oxide** layer thickness decreases with the increase of SiC content.
- A SiC content <5 vol.% is not sufficient in aiding the protection of fibres at 1650 °C in air.
- A SiC content >15 vol.% provides full protection of the fibres during oxidation up to 1650 °C.

Abstract

The microstructure and the oxidation resistance in air of continuous carbon fibre reinforced ZrB₂-SiC ceramic composites were investigated. SiC content was varied between 5–20 vol.%, while maintaining fibre content at ~40 vol.%. Short term oxidation tests in air were carried out at 1500 and 1650 °C in a bottom-up loading furnace. The thickness, composition and microstructure of the resulting oxide scale were analysed by SEM-EDS and X-Ray diffraction. The results show that contents above 15 vol.% SiC ensure the formation of a homogeneous protective borosilicate glass that covers the entire sample and minimizes fibre burnout. The scale thickness is ~90 µm for the sample containing 5 vol.% SiC and decreases with increasing SiC content.

[< Previous article](#)

[Next article >](#)

Keywords

Ceramic-matrix composites (CMCs); Ultra-High-Temperature-Ceramics (UHTCs); Oxidation resistance; Microstructure; Carbon fibre

1. Introduction

The [borides](#) of early [transition metals](#) are covalent compounds characterized by melting points exceeding 3000 °C and are part of a class of materials called Ultra High Temperature Ceramics (UHTCs). They display high thermal and electrical conductivity and good ablation resistance [\[\[1\], \[2\], \[3\]\]](#) Among UHTCs, ZrB₂ has been extensively studied as a potential candidate for the fabrication of reusable Thermal Protection Systems (TPS) for aerospace applications or for use in hypersonic aircrafts [\[4,5\]](#) owing to its high [thermal conductivity](#) and relatively low density [\[1,6,7\]](#). The main drawbacks of these materials are their low fracture toughness and poor [thermal shock resistance](#) which constitute major problems to their implementation [\[8\]](#). Moreover, the [oxidation resistance](#) of monolithic ZrB₂ is low at temperatures above 1200 °C due to the formation of volatile [oxides](#) (B₂O₃) and of a porous ZrO₂ scale which does not provide protection against further oxidation [\[9\]](#). The addition of silicides, such as SiC or MoSi₂, has been found to aid the [sintering](#) of ZrB₂ and to increase its oxidation resistance due to the formation of a viscous [borosilicate glass](#) with low vapour pressure [\[\[10\], \[11\], \[12\], \[13\]\]](#)

C/C and C/SiC composites currently used in aerospace applications are characterized by good [thermo-mechanical properties](#), low thermal expansion, low density and good thermal shock resistance. However, in C/C composites the [carbon fibres](#) undergo oxidation already at 500 °C, while in C/SiC or SiC/SiC composites the protective layer of liquid SiO₂, originating from the oxidation of SiC matrix at 1100 °C, becomes chemically active above 1650 °C, leading to high removal rates [\[\[14\], \[15\], \[16\]\]](#).

Several approaches have been materials and overcome their respective weaknesses. One method involves the reinforcing of C/C composites with UHTC particles by dispersing the latter in the phenolic [resin](#) and then infiltrating the carbon fabrics which in turn leads to increased ablation and oxidation resistance [\[4, 14, 15\]](#)

Another approach involves the coating of C/C composites with a layer of UHTC phase in order to retain the mechanical properties provided by the carbon substrate and exploit the ablation and oxidation resistance provided by the coating. Common issues are coating spallation deriving from the CTE mismatch between the two materials. In this regard, Corral et al. have been able to achieve a good interface between the carbon substrate and the UHTC coating and demonstrated the increased oxidation resistance at T > 1600 °C [\[\[16\], \[17\], \[18\], \[19\]\]](#).

However, all the aforementioned approaches introduce only a little percentage of the UHTC phase in the final material. Some works have been done on UHTCs reinforced with carbon spheres or short fibres [[20], [21], [22], [23]], but there are very few works concerning the performance of continuous fibre reinforced composites with a UHTC-rich matrix under oxidizing atmospheres. Sciti and Zoli have successfully obtained carbon fibre reinforced UHTCs via slurry infiltration and hot pressing [24,25]. The main problem in the manufacturing of these composites is usually associated to the difficult infiltration of the fibre preforms [24] and the sintering process [25] that can severely damage the fibres. Preliminary studies on these materials have shown their promising mechanical properties and oxidation resistance at 1500 °C [26,24]. Recent studies on the kinetics of oxidation of a carbon fibre reinforced ZrB₂ composite doped with 10 vol.% SiC have shown that the critical temperature for these composites is below 1000 °C, where the formation of a protective borosilicate scale is slow and not effective and the fibres get excessively damaged. However, at temperatures above 1200 °C a borosilicate glass forms at an appreciable rate and quickly protects the underlying fibres, preventing further oxidation of the material [13].

Previous studies on the effect of different oxygen partial pressures on the oxidation resistance of ZrB₂ ceramics doped with 20% and 30% SiC have shown that higher SiC contents are beneficial in oxygen-rich environments but the effect is reversed in oxygen-poor atmospheres due to the active oxidation of SiC to SiO_(g) [27]. The latter issue has raised many concerns regarding the use of SiC in ceramic composites.

However, the majority of these works has been carried out on bulk ceramics with high SiC contents (>20 vol.%) [[28], [29], [30], [31]]. There is still a limited amount of literature on the oxidation resistance of low SiC-bearing UHTC composites reinforced with fibres and how the fibre orientation influences oxidation depending on the final application. Moreover for fibre reinforced ceramics the amount of readily available SiC is actually halved, since ~50% of the composite is constituted by the fibre reinforcement.

In the present work carbon fibre reinforced ZrB₂-SiC composites were fabricated by slurry infiltration and hot pressing. SiC was added in amounts ranging from 5 to 20 vol.% of the ceramic matrix and the oxidation resistance was evaluated at 1500 and 1650 °C in air. The samples were exposed directly to the target temperature for short times in order to bypass the critical temperature of 1000 °C and trigger the oxidation of SiC to SiO₂ [13].

2. Experimental

2.1. Materials

Commercially available powders were used for the fabrication of ceramic composite materials: ZrB₂ (H.C. Starck, grade B, Germany, specific surface area 1.0 m²/g, particle size range 0.5–6 µm, impurities (wt.%): 0.25 C, 2 O, 0.25 N, 0.1 Fe, 0.2 Hf), α-SiC (H.C. Starck, Grade UF-25, Germany, specific surface area 23–26 m²/g, D50 0.45 µm Italian retailer: Metalchimica). Unidirectional high modulus carbon fibre fabrics (Granoch, Yarn XN80-6 K fibres; tensile modulus of 780 GPa and tensile strength 3.4 GPa, 10 µm fibre diameter. Supplier: G. Angeloni) were used as carbon preforms.

2.2. Process

Powder mixtures containing ZrB₂ and SiC ranging from 5 to 20 vol.% were prepared by wet ball-milling of the commercial powders and then dried with a rotary evaporator. The composites were prepared through slurry infiltration of unidirectional carbon fibre preforms and hand lay-up in a 0–90° configuration. Hot pressing was carried out at 1900 °C, under a uniaxial pressure of 40 MPa and an holding time of 10 min, on the basis of previous studies [25]. Four specimens containing SiC in amounts ranging between 5 and 20 vol.% were fabricated by adjusting the powder suspension rheology accordingly. Due to the intrinsic variance of the manual process, it was not possible to obtain the same exact fibre contents for all samples. Since the values remain within the 5% scattering, they were considered comparable for this study.

2.3. Microstructure analysis

The microstructure and elemental composition were analysed on polished and fractured surfaces by field emission scanning electron microscopy (FE-SEM, Carl Zeiss Sigma NTS GmbH Oberkochen, Germany) and energy dispersive x-ray spectroscopy (EDS, INCA Energy 300, Oxford instruments, UK). Specimens for microscopy were prepared by

cutting cross sections, mounting them in epoxy resin and polishing them down to a 0.25 µm finish with diamond abrasives, using semi-automatic polishing machine (Tegramin-25, Struers, Italy). The polished samples were then washed with ethanol and acetone in an ultrasonic bath, dried under IR light and cleaned with a plasma cleaner (Colibri Plasma RF 50 KHz, Gambetti, Italy) at 40 W for 5 min. For the oxidized samples, a thin carbon coating was applied with a turbo-pumped sputter coater (Q150T, Quorum Technologies Ltd, UK) on the surface of the specimens to avoid electron scattering on the insulating oxides during SEM analysis.

The fibre volumetric amount was determined by taking into account the fibre areal weight (g/m²) given by the supplier, number of layers and sample area. The matrix amount was then determined as the difference between the total pellet weight and the fibre weight. The theoretical density of the materials based on the initial composition was calculated using the rule of mixture. The mean grain size of ZrB₂ was evaluated via image analysis with the software Image-Pro Analyser 7.0, following the standard ISO 13383-1, method A2. X-Ray diffraction analysis was carried out on the samples oxidized at 1500 and 1650 °C using a Bruker D8 Advance apparatus (Bruker, Karlsruhe, Germany).

2.4. Oxidation tests

Regular bars with dimensions 2.5 × 2 × 12 mm (Width × Thickness × Length) were machined from the sintered pellet. The samples were cleaned with acetone in an ultrasonic bath and dried at 100 °C. The oxidation tests were carried out in a bottom-up loading furnace (FC18-0311281, Nannetti Antonio Sauro S.R.L., Italy) at 1500 and 1650 °C in air for 1 min. The furnace was heated to the target temperature with a rate of 5 °C/min. Then the specimens were introduced in the furnace using a porous alumina sample holder. After reaching thermal equilibrium (30 s), the sample was kept in the furnace for 1 min. At the end of the oxidation test, the specimens were quickly taken out and let to cool down naturally in air. For the test at 1650 °C, an additional minute was needed to reach thermal equilibrium.

3. Results and discussion

3.1. Microstructure of the sintered material

In Table 1 the physical properties of samples ZS5-20 are reported. UHTC composites are usually difficult to sinter due to the low diffusivity of ZrB₂ and the presence of large amounts of fibres that constrain the matrix shrinkage. A porosity of ~5 vol.% was obtained only for the sample with a SiC content of 20 vol.%, owing to SiC capability of aiding the sintering of ZrB₂ via liquid phase sintering [32,33]. There is also a slight decrease of the ZrB₂ grain size associated with the increase of SiC content, which is consistent with the results obtained by Fahrenholtz et al. [34].

Table 1. Physical properties of samples ZS5, ZS10, ZS15, ZS20.

	ZS 5	ZS 10	ZS 15	ZS 20
Density (g/cm³)	3.65	3.86	3.95	4.00
Porosity (vol. %)	12.9	9.8	7.5	5.4
Fibre (vol. %)	40	38	37	37
ZrB₂ grain size (µm)	~3.4	~2.8	~2.5	~2.0

In Fig. 1 the low magnification micrograph of sample ZS10 is shown as an example. The black dots and lines represent the carbon fibres stacked in a 0/90° configuration, while the light phase is the UHTC matrix.

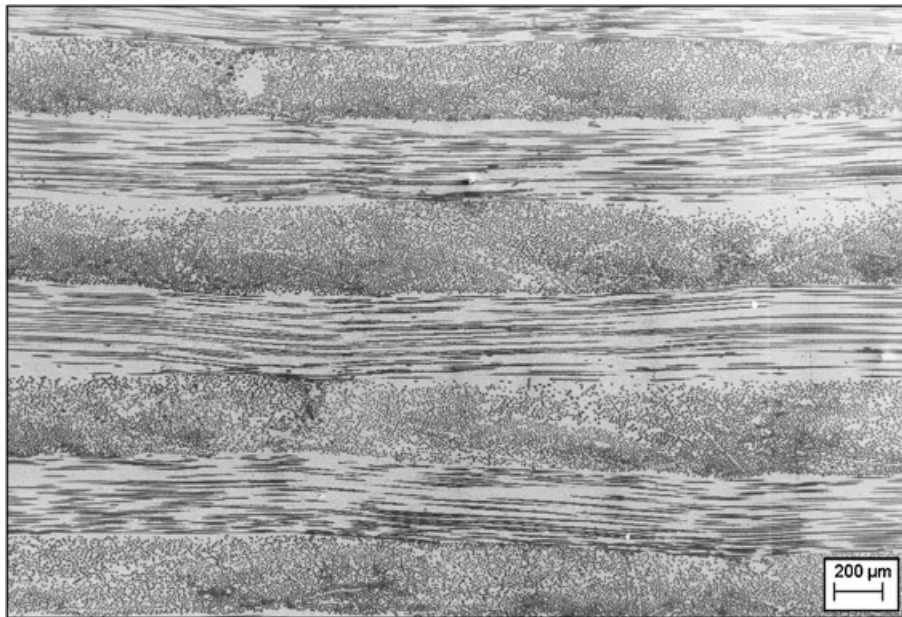
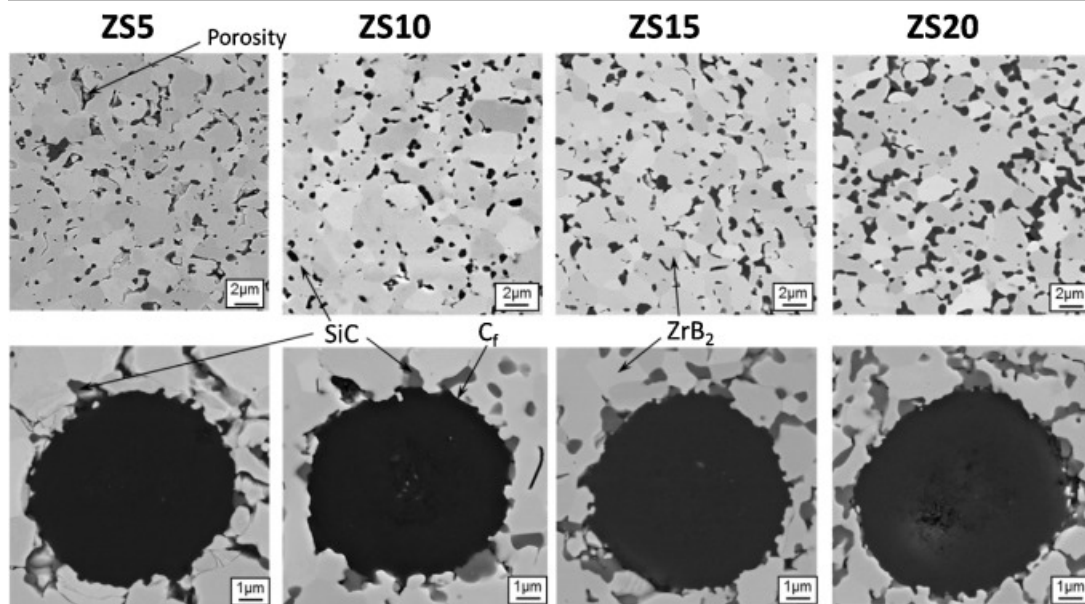


Fig. 1. Low magnification micrograph of sample ZS10 showing the 0/90° configuration of the carbon fibre layers (black) infiltrated with the UHTC matrix (white).

Samples manufactured with this process may be characterized by non-infiltrated areas and cracks in the matrix-rich regions which originate from the constrained shrinkage of the ceramic matrix during sintering and the mismatch between the thermal expansion coefficients of the matrix and fibres ($6.5 \cdot 10^{-6} \text{ K}^{-1}$, $2 \cdot 10^{-6} \text{ K}^{-1}$, respectively [9]).

In our case it was possible to obtain the homogenous infiltration of the fibres in all samples. In Fig. 2 the high magnification micrographs of samples ZS5-20 are reported. The light and dark grey phases represent ZrB₂ and SiC respectively, while the carbon fibre is black.



[Download high-res image \(778KB\)](#) [Download full-size image](#)

Fig. 2. High magnification micrographs of samples ZS5, ZS10, ZS15, ZS20. The top micrograph shows the microstructure of the ceramic matrix where the dark phases represent SiC and porosity while the light grey is ZrB₂. The bottom micrograph shows the polished cross section of the carbon fibre.

SiC particles are well dispersed in the ZrB₂ matrix but for contents above 15 vol. % they tend to agglomerate. The sample containing 5 vol. % SiC is characterized by a higher degree of porosity which decreases with the increase of SiC content. In all samples the fibres do not show significant signs of reaction with the surrounding ceramic matrix and maintain their original round shape, which is in agreement with previous studies on carbon fibre reactivity done by Silvestroni et al. [35].

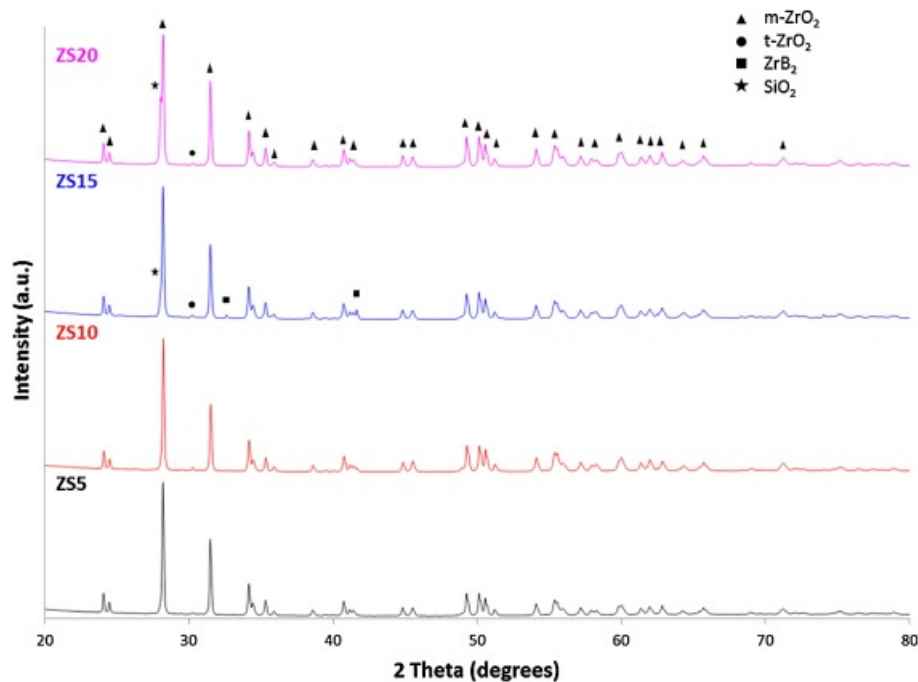
3.2. Oxidation tests

Samples were weighed before (w_{in}) and after (w_{fin}) oxidation cycles and the weight difference was normalized over the initial surface area, S ($\frac{\Delta m}{S} = \frac{w_{fin} - w_{in}}{S}$). Although there were slight variations in the sample compositions and fibre content, and therefore the individual values were not perfectly comparable, all samples underwent weight loss after oxidation at 1500 and 1650 °C. Weight loss was notably higher at 1650 than at 1500 °C, except for sample ZS20 for which it was unchanged. (Table 2).

Table 2. Mass variation normalized to the surface area after oxidation tests at 1500 and 1650 °C for samples ZS5-20.

	ZS5	ZS10	ZS15	ZS20
$\Delta m/S_{1500\text{ °C}}$ (mg/cm ²)	-1.9	-1.9	-3.6	-2.4
$\Delta m/S_{1650\text{ °C}}$ (mg/cm ²)	-3.9	-3.6	-7.0	-2.3

X-Ray diffraction was carried out on the surface layer of the samples after oxidation at 1500 and 1650 °C. At 1500 °C (Fig. 3) the predominant phase is monoclinic zirconia (PDF 83–0939) with trace amounts of tetragonal zirconia (PDF 88-1007); there is a small peak arising at 28 2-theta attributed to crystalline SiO₂ species (PDF 82–1559) that increases with the increase of SiC content. For the sample ZS15, a peak relative to ZrB₂ (PDF 75–1050) was also observed; this could be attributed to a locally damaged oxide scale which exposed the unreacted matrix.

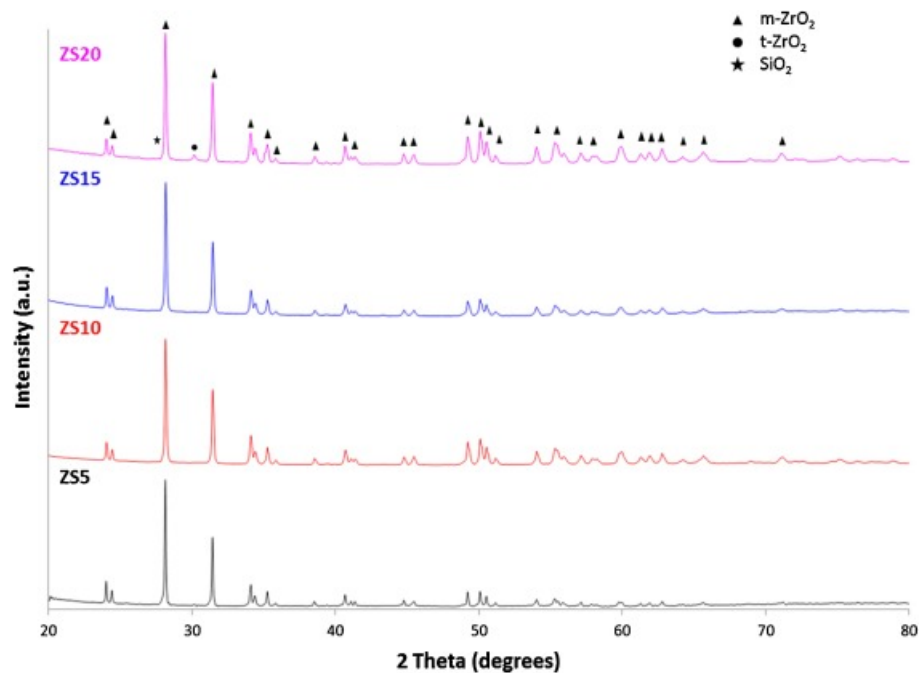


[Download high-res image \(207KB\)](#) [Download full-size image](#)

Fig. 3. X-Ray diffraction patterns of the surface of samples ZS5, ZS10, ZS15, ZS20 oxidized at 1500 °C in air.

In previous studies on the oxidation of a ZrB₂ bulk ceramic doped with 20 vol. % of SiC, Gao et al. found evidence of the formation of zirconium silicate (ZrSiO₄) between 1200 and 1500 °C both at low and high oxygen partial pressure, highlighting that the zircon yield was higher in oxygen-poor atmosphere [36]. In our case no formation of zircon was observed at 1500 °C. This could be explained both by the short exposure times, the oxygen-rich atmosphere and the overall lower SiC content.

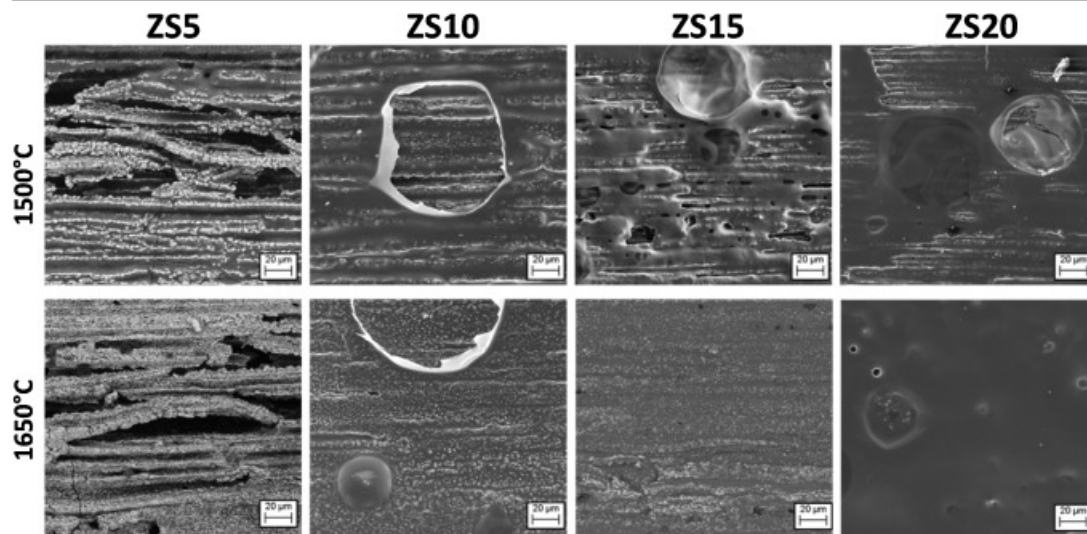
At 1650 °C (Fig. 4) only the peaks relative to monoclinic zirconia could be seen while no SiO₂ platelets were detected on the surface, in agreement with the aforementioned work [36]. This was attributed to the evaporation of the outer borosilicate layer which leaves behind only amorphous phases not detected by X-ray diffraction. The peaks relative to tetragonal zirconia were observed only in sample ZS20. No phases relative to carbon or the formation of carbides were observed.



[Download high-res image \(195KB\)](#) [Download full-size image](#)

Fig. 4. X-Ray diffraction patterns of the surface of samples ZS5, ZS10, ZS15, ZS20 oxidized at 1650 °C in air.

Following the XRD characterization, SEM analysis was carried out on the surface and cross section of the oxidized samples. A top view of the surface of specimens ZS5-20 oxidized at 1500 °C and 1650 °C is shown in Fig. 5. It is possible to observe the formation of bubbles which are due to the evolution of volatile oxides that will be discussed in detail later.

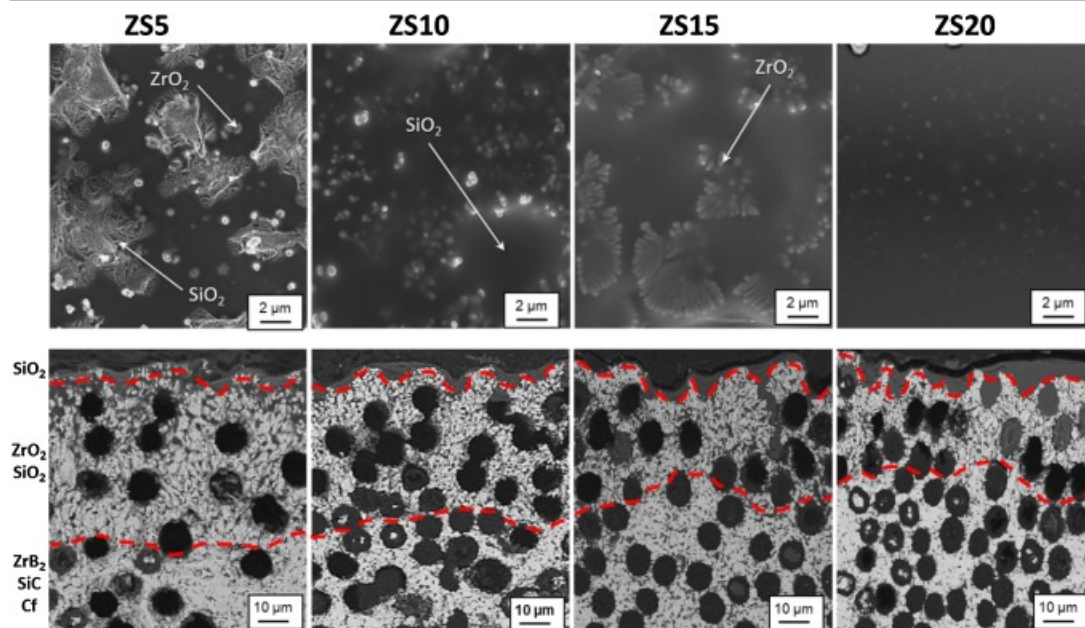


[Download high-res image \(932KB\)](#) [Download full-size image](#)

Fig. 5. Top view of the oxidized samples at 1500 °C (top) and 1650 °C (bottom). The white area are constituted mainly by monoclinic sub-micrometric ZrO₂, while the dark grey zones consist mainly of amorphous borosilicate glass.

The samples containing a higher amount of SiC (ZS15 and ZS20) are the ones characterized by a higher amount of blisters on the surface; this is associated with the greater amount of liquid phase formed during the oxidation of SiC to SiO_{2(l)}. The specimen containing 5 vol. % SiC is visibly the most damaged. Moreover it is possible to notice that for the samples containing intermediate amount of SiC the oxidation is not homogeneous but takes place locally with the formation of silica channels, preferentially in the hollows left by the oxidation of the outer fibres.

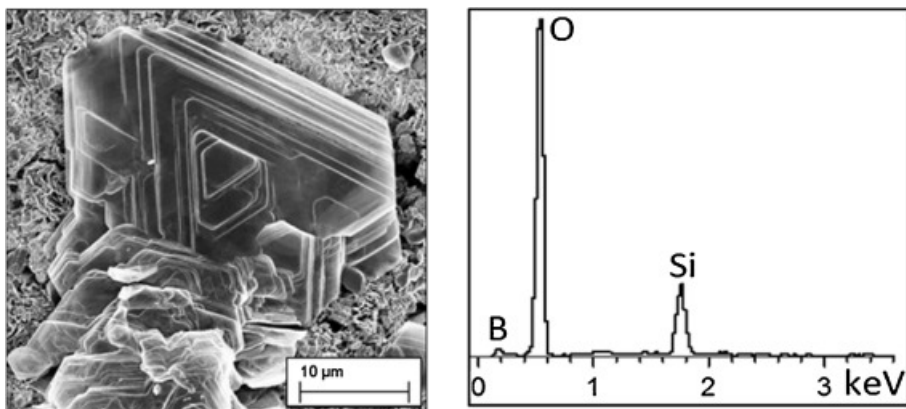
In Fig. 6, the high magnification micrographs of the surface and the cross section of samples ZS5-20 oxidized at 1500 °C is shown. The rapid exposition to high temperatures effectively limits the oxidation of fibres which is critical at 1000 °C [13]. Sample ZS5 is characterized by the lowest amount of SiC which is reflected in the lowest amount of silica glass formed during oxidation. Large ZrO₂ grains emerging from the glassy phase were observed. With the increase of SiC content it is possible to see the progressive coverage of the surface with a liquid borosilicate glass that fills the holes left by the outer fibre burnout and prevents further oxygen diffusion inside the material. The small white dots that can be seen in transparency are precipitated ZrO₂ grains in the borosilicate glass. At high temperature, the B₂O₃ partially dissolves the ZrO₂ but with the increase of SiC content, the size and amounts of precipitated zirconia decreases because the glassy phase becomes progressively impoverished of B₂O₃ [28].



[Download high-res image \(1MB\)](#) [Download full-size image](#)

Fig. 6. High magnification micrographs of the surface (top) and cross section (bottom) of the oxidized samples at 1500 °C. The dark and light grey phases represent SiO₂ and ZrO₂ respectively. The holes (black) are due to fibre burnout.

Closely inspecting the surface of sample ZS5 oxidized at 1500 °C, some platelets were observed and EDS analysis suggested their chemical composition (Fig. 7), most likely originating from the cooling down of the boron-rich borosilicate melt.



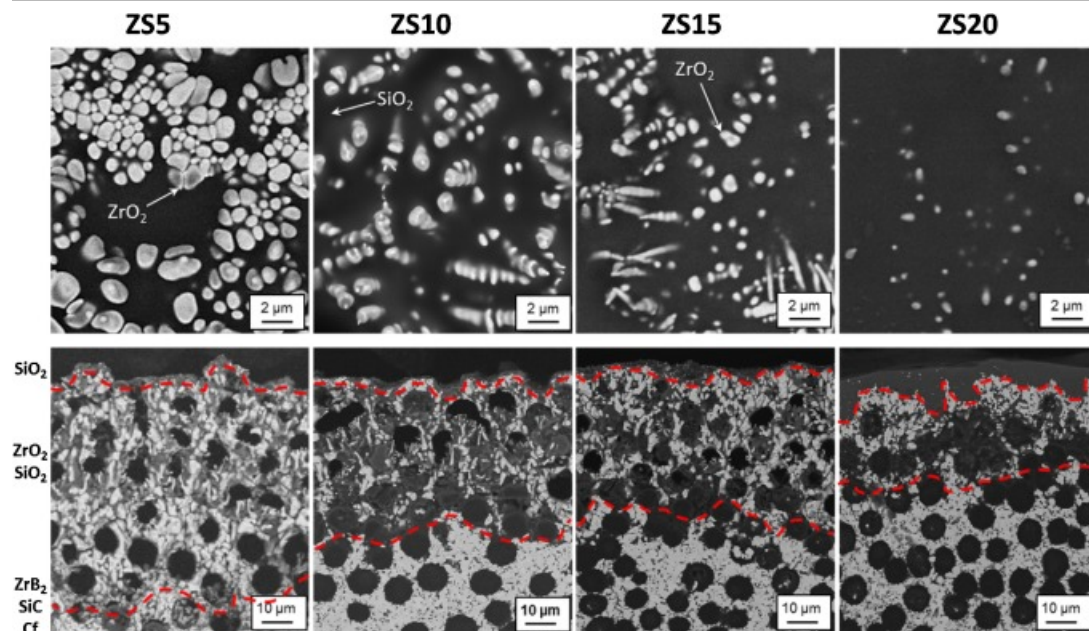
[Download high-res image \(389KB\)](#) [Download full-size image](#)

Fig. 7. Platelets of B₂O₃-SiO₂ formed on the surface of sample ZS5 after oxidation at 1500 °C in air.

The cross section is characterized by three distinct layers: 1) an external borosilicate glass layer, 2) an intermediate zirconia-silica scale, where the holes left by the fibre oxidation are partially filled by silica, 3) unreacted matrix scale. The thickness of the oxidized layer slightly decreases with the increase of SiC content but remains in the range of 40–60 μm.

Previously Fahrenholtz studied and thoroughly discussed the formation of a SiC-depleted layer between the ZrO₂/SiO₂ scale and the unreacted matrix in a ZrB₂/SiC ceramic originating from the active oxidation of SiC to form volatile SiO [37]. The same author also investigated the influence of [graphite](#) addition in a ZrB₂/SiC composite and found out that the presence of carbon may lead to the preferential formation of CO which lowers the SiO partial pressure and allows to retain the SiC phase [20]. Assuming that the highly graphitic fibres used in this work have a similar reactivity to graphite, this could justify the lack of a SiC-depleted layer in our oxidized samples.

After oxidation at 1650 °C the samples appear visibly more damaged ([Fig. 8](#)). The zirconia grains, which were barely visible at 1500 °C, are now exposed due to the partial evaporation of the outer silica layer. Sample ZS5 is characterized by large ZrO₂ particles on the surface, while the inner layer is thicker, more fragmented and porous. Samples ZS10 and ZS15 show very similar microstructure; dendritic zirconia can be observed growing in the glassy phase, but a good amount of silica glass is still present. Sample ZS20 is the least affected by the oxidation at 1650 °C and the oxidized layer thickness is almost unchanged (35 μm), which is also reflected in the constant weight loss ([Table 2](#)). The sample is still fully covered by silica and the only observable changes are a higher amount of blisters on the surface and the appearance of ZrO₂ needles from below.



[Download high-res image \(1MB\)](#) [Download full-size image](#)

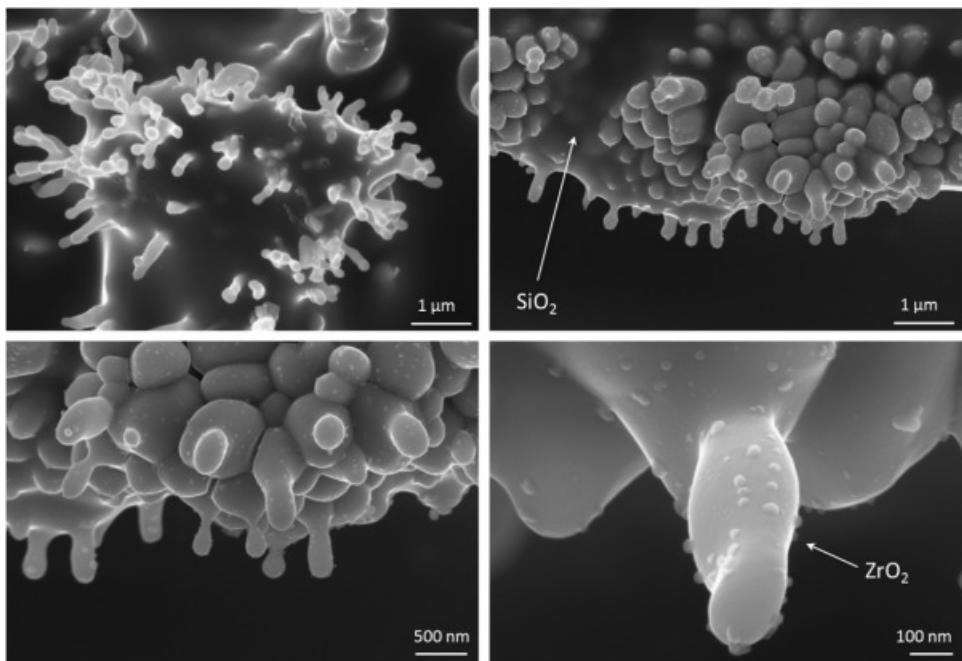
Fig. 8. High magnification micrographs of the surface (top) and cross section (bottom) of the oxidized samples at 1650 °C. The dark and light grey phases represent SiO₂ and ZrO₂ respectively. The holes (black) are due to fibre oxidation.

The thicknesses of the oxidized layer for samples ZS5-20 shown in Table 3 tend to decrease with the increase of SiC content and for sample ZS15 and ZS20 are almost unchanged for the tests at 1500 and 1650 °C.

Table 3. Average values of thickness of the oxidized layer (outer SiO₂/B₂O₃ layer + ZrO₂/SiO₂ scale) at 1500 and 1650 °C for samples ZS5-20.

	ZS5	ZS10	ZS15	ZS20
Oxide thickness 1500 °C (μm)	64	50	45	36
Oxide thickness 1650 °C (μm)	85	57	50	35

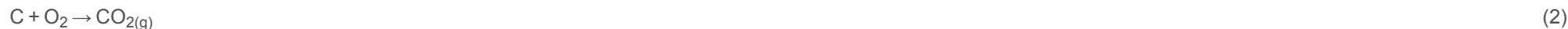
Further inspection on the small zirconia crystals found underneath the ruptured bubbles allowed to detect a coral-like structure (Fig. 9). These crystals are immersed in a glassy scale that was identified predominantly as SiO₂ by EDS. On the tip and the sides of these needles it is possible to observe the growth of small nuclei that remind the branches of a dendrite. This type of dendritic zirconia was previously described by Halloran et al. as secondary zirconia crystals that precipitate from the molten borosilicate glass where they were dissolved [28,38]



[Download high-res image \(622KB\)](#) [Download full-size image](#)

Fig. 9. High magnification micrographs of secondary zirconia growing under the ruptured bubbles of sample ZS20 oxidized at 1500 °C. The dark and light grey phases represent SiO₂ and ZrO₂ respectively.

Previous studies on the kinetics of oxidation of a carbon fibre reinforced ZrB₂/SiC composite concluded that the overall oxidation behaviour of these materials at temperatures from 800 to 1400 °C is the result of two competing phenomena; on one hand the weight loss due to fibre burnout (Reactions (1) and (2) and on the other the weight gain due to oxidation of ZrB₂ and SiC (Reactions (3) and (4)

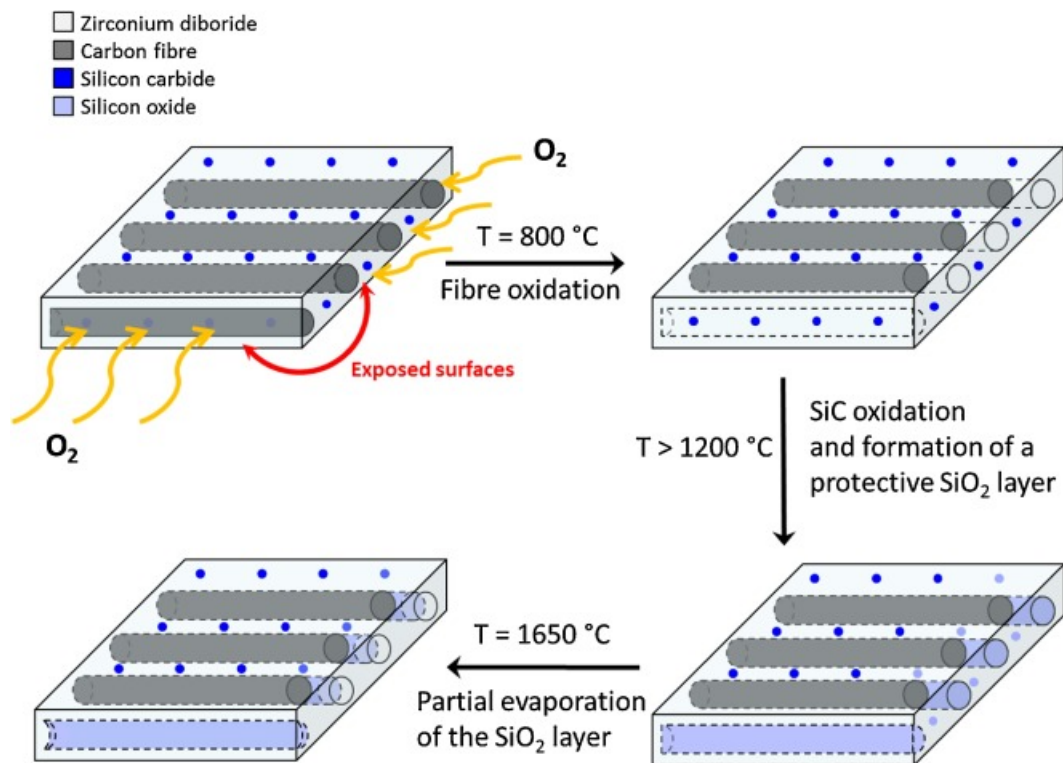


Reaction (3) begins at $T > 800$ °C whilst formation of borosilicate glass starts at $T > 1200$ °C. The faster is the formation of a protective borosilicate layer, the slower is the fibre oxidation [39]. The most critical temperature range is between 800 and 1200 °C, because there is no protective layer on the surface, apart from some poorly effective liquid B₂O₃. At temperatures higher than 1200 °C, formation of the borosilicate glass starts to protect the fibre from further oxidation and their oxidation is progressively halted.

The overall oxidation mechanisms for the present materials can be explained as follows. During introduction of the coupons inside the hot chamber, the samples experience an abrupt increase of temperature from RT to 1500 °C or 1650 °C. Although the permanence at the critical temperature range between 700 °C and 1200 °C is estimated to be ~10 s, this short time is enough for burning out of first layer of fibres, according to Reactions (1) and (2). Then it is reasonable to speculate that formation of the borosilicate layer forming at $T > 1200$ °C starts to slow down the oxygen diffusion by filling the cavities left by the burnt carbon fibres and covering the matrix surface. The effect of heating rate was already investigated and proven to minimize fibre oxidation by triggering the faster formation of a glassy phase [39]. The glass formation is more abundant for higher amounts of SiC which is consistent with the progressively thicker silica scale but overall thinner oxide scale (Fig. 8).

The overall mass loss after oxidation (Table 2) can be attributed to the harsher conditions of these tests compared to those carried out in the thermo-gravimetric analyser. The exposure to air for 1 min at 1500 °C in the bottom-up furnace led to almost the same degree of oxidation of the equivalent TGA test carried out up to 1550 °C in the span of 2.5 h. The increased oxidation rate can be ascribed to the non-static air of the bottom-up furnace used in this experiment; during the introduction of the sample inside the furnace, cold air enters the chamber and, upon heating, gives rise to turbulent flow which contributes to material removal from the surface of the specimen.

Moreover since the oxidation tests were carried out on small bars, the specimens underwent oxidation both on the surface and on the sides. For the application as thermal protection systems for the leading edges of aerospace vehicles, where fibres normally do not face outwards, only the outer surface of the tile would be exposed to the corrosive atmosphere [40]. The results obtained in this work also account for potential oxidation phenomena that may take place on the sides of the specimen (e.g. as a result of a crack or defect and subsequent exposure of the underlying material, or when used for the fabrication of nozzle inserts where multiple fibre orientations may be chosen). The oxidation of fibre reinforced composites for fibres exposed to air parallel and perpendicular to the fibre axis is schematized in Fig. 10.

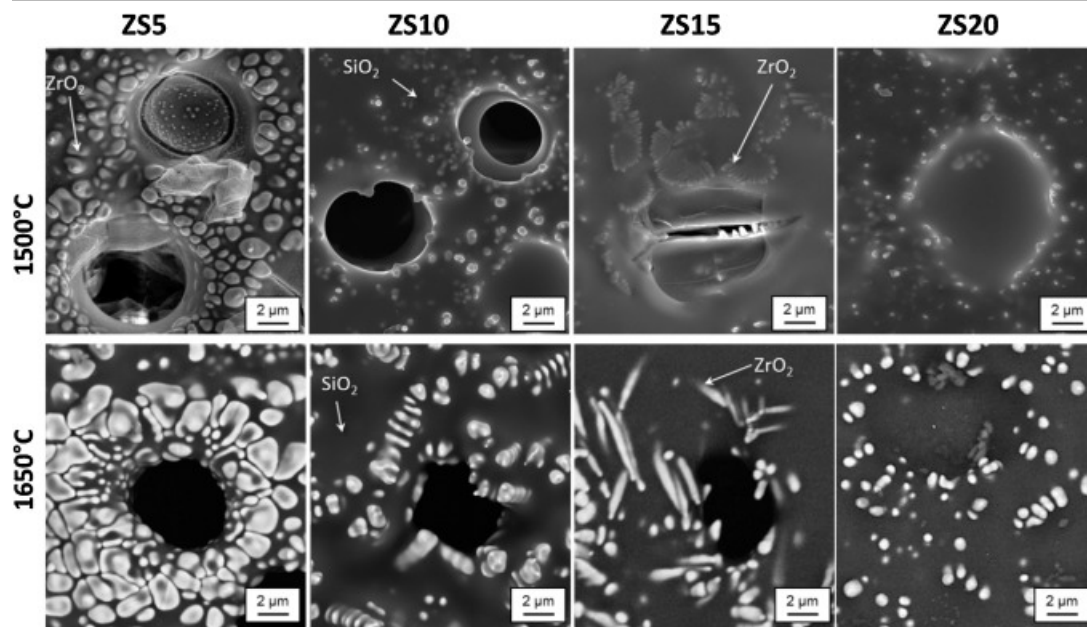


[Download high-res image \(532KB\)](#)

[Download full-size image](#)

Fig. 10. Model for the lateral oxidation of fibres exposed to air parallel and perpendicular to the fibre axis: initially the outer fibres completely burn while the inner fibres get partially oxidized. Then the SiC from the matrix turns to liquid SiO₂ that fills the holes left by the oxidation of the fibres. At 1650 °C the silica layer partially evaporates.

If the side of the fibres is exposed, which is what happens on the surface as discussed before, the outer fibres readily burn and leave behind a layer of continuous ceramic matrix that behaves like a conventional bulk ceramic. On the other hand, if the fibre section is exposed, the oxidation of carbon results in the formation of channels that favour further diffusion of oxygen inside the material. In this case, the increasing amount of SiC leads to the progressive coverage of the holes left by the fibre oxidation in the section which ultimately results in the halted oxidation of the material (Fig. 11).



[Download high-res image \(788KB\)](#) [Download full-size image](#)

Fig. 11. High magnification micrographs of the lateral section of the oxidized samples at 1500 and 1650 °C. The dark and light grey phases represent SiO₂ and ZrO₂ respectively. The holes (black) are due to fibre burnout.

4. Conclusions

The influence of SiC content on the [oxidation resistance](#) in air of fibre reinforced ZrB₂-SiC composites was investigated at 1500 and 1650 °C. The rapid exposure to high temperature triggers the quick formation of a [borosilicate](#) layer which prevents further oxidation of the underlying fibres. For SiC content <5 vol.%, the formation of the protective glass is not sufficient and this leads to excessive local burnout of the fibres, ultimately resulting in the rupture of the [oxide](#) layer. Moreover the higher degree of porosity promotes the inward diffusion of oxygen and further oxidation of the material. For SiC >15 vol.%, the borosilicate layer covers the entire sample and this results in increased oxidation resistance. The formation of blisters due to the evolution of volatile oxides was observed.

The oxidation is not homogeneous and depends on the layer configuration: when the oxidation takes place orthogonal to the [fibres orientation](#), the latter completely burn and expose a continuous layer of ceramic matrix that behaves like a conventional ceramic. When the oxidation takes place parallel to the fibre orientation, channels are created through which oxygen can diffuse inside the materials. The oxidation of the fibres eventually comes to an halt when a sufficient amount of liquid glassy phase forms and covers the sample.

At 1650 °C the outer glassy phase partially evaporates, exposing dendritic [zirconia](#) precipitated from the [molten borosilicate glass](#). The thickness of the oxidized layer decreases with the increase of SiC content at all temperatures. The sample containing 20 vol.% SiC in the matrix is the least affected by oxidation and gets effectively

passivated with no relevant changes to the microstructure and the weight loss. From the results obtained so far, a SiC content >15 vol% is sufficient to provide the full coverage of the sample in oxygen-rich environments and provide protection to the underlying fibres.

Further research on the oxidation resistance at low oxygen partial pressure and at higher temperatures has to be carried out in order to study the effect of SiC and the presence of [carbon fibres](#) in the ZrB₂ matrix.

Acknowledgement

This work has received funding from the European Union's Horizon 2020 "Research and innovation programme" under grant agreement No [685594](#) (C³HARME).

[Recommended articles](#)

Citing articles (0)

References

- [1] M.M. Opeka, I.G. Talmy, E.J. Wuchina, J.A. Zaykoski, S.J. Causey
Mechanical, thermal, and oxidation properties of refractory hafnium and zirconium compounds
J. Eur. Ceram. Soc., 19 (1999), pp. 2405-2414, [10.1016/S0955-2219\(99\)00129-6](https://doi.org/10.1016/S0955-2219(99)00129-6)
[Article](#)  [Download PDF](#) [View Record in Scopus](#) [Google Scholar](#)
- [2] S. Tang, J. Deng, S. Wang, W. Liu
Comparison of thermal and ablation behaviors of C/SiC composites and C/ZrB₂-SiC composites
Corros. Sci., 51 (2009), pp. 54-61, [10.1016/j.corsci.2008.09.037](https://doi.org/10.1016/j.corsci.2008.09.037)
[Article](#)  [Download PDF](#) [View Record in Scopus](#) [Google Scholar](#)
- [3] W.W. Wu, M. Estili, T. Nishimura, G.J. Zhang, Y. Sakka
Machinable ZrB₂-SiC-BN composites fabricated by reactive spark plasma sintering
Mater. Sci. Eng. A, 582 (2013), pp. 41-46, [10.1016/j.msea.2013.05.079](https://doi.org/10.1016/j.msea.2013.05.079)
[Article](#)  [Download PDF](#) [View Record in Scopus](#) [Google Scholar](#)
- [4] A. Paul, J. Binner, B. Vaidyanathan
UHTC composites for hypersonic applications
Ultra-High Temp. Ceram. Mater. Extrem. Environ. Appl. (2014), pp. 144-166, [10.1002/9781118700853.ch7](https://doi.org/10.1002/9781118700853.ch7)
[CrossRef](#) [View Record in Scopus](#) [Google Scholar](#)
- [5] A. Cecere, R. Savino, C. Allouis, F. Monteverde
Heat transfer in ultra-high temperature advanced ceramics under high enthalpy arc-jet conditions
Int. J. Heat. Mass. Transf., 91 (2015), pp. 747-755, [10.1016/j.ijheatmasstransfer.2015.08.029](https://doi.org/10.1016/j.ijheatmasstransfer.2015.08.029)
[Article](#)  [Download PDF](#) [View Record in Scopus](#) [Google Scholar](#)
- [6] S.R. Levine, E.J. Opila, M.C. Halbig, J.D. Kiser, M. Singh, J.A. Salem
Evaluation of ultra-high temperature ceramics for aeropulsion use

J. Eur. Ceram. Soc., 22 (2002), pp. 2757-2767, [10.1016/S0955-2219\(02\)00140-1](https://doi.org/10.1016/S0955-2219(02)00140-1)

[Article](#)  [Download PDF](#) [View Record in Scopus](#) [Google Scholar](#)

[7] F. Monteverde, S. Guicciardi, A. Bellosi

Advances in microstructure and mechanical properties of zirconium diboride based ceramics

Mater. Sci. Eng. A, 346 (2003), pp. 310-319, [10.1016/S0921-5093\(02\)00520-8](https://doi.org/10.1016/S0921-5093(02)00520-8)

[Article](#)  [Download PDF](#) [View Record in Scopus](#) [Google Scholar](#)

[8] J.J. Sha, J. Li, S.H. Wang, Z.F. Zhang, Y.F. Zu, S. Flauder, W. Krenkel

Improved microstructure and fracture properties of short carbon fiber-toughened ZrB₂-based UHTC composites via colloidal process

Int. J. Refract. Met. Hard Mater., 60 (2016), pp. 68-74, [10.1016/j.ijrmhm.2016.07.010](https://doi.org/10.1016/j.ijrmhm.2016.07.010)

[Article](#)  [Download PDF](#) [View Record in Scopus](#) [Google Scholar](#)

[9] W.G. Fahrenholtz, G.E. Hilmas, I.G. Talmy, J.A. Zaykoski

Refractory diborides of zirconium and hafnium

J. Am. Ceram. Soc., 90 (2007), pp. 1347-1364, [10.1111/j.1551-2916.2007.01583.x](https://doi.org/10.1111/j.1551-2916.2007.01583.x)

[CrossRef](#) [View Record in Scopus](#) [Google Scholar](#)

[10] T.A. Parthasarathy, R.A. Rapp, M. Opeka, R.J. Kerans

A model for the oxidation of ZrB₂, HfB₂ and TiB₂

Acta Mater., 55 (2007), pp. 5999-6010, [10.1016/j.actamat.2007.07.027](https://doi.org/10.1016/j.actamat.2007.07.027)

[Article](#)  [Download PDF](#) [View Record in Scopus](#) [Google Scholar](#)

[11] L. Silvestroni, G. Meriggi, D. Sciti

Oxidation behavior of ZrB₂ composites doped with various transition metal silicides

Corros. Sci., 83 (2014), pp. 281-291, [10.1016/j.corsci.2014.02.026](https://doi.org/10.1016/j.corsci.2014.02.026)

[Article](#)  [Download PDF](#) [View Record in Scopus](#) [Google Scholar](#)

[12] L. Zoli, D. Sciti

Efficacy of a ZrB₂-SiC matrix in protecting C fibres from oxidation in novel UHTCMC materials

Mater. Des., 113 (2017), pp. 207-213, [10.1016/j.matdes.2016.09.104](https://doi.org/10.1016/j.matdes.2016.09.104)

[Article](#)  [Download PDF](#) [View Record in Scopus](#) [Google Scholar](#)

[13] A. Vinci, L. Zoli, E. Landi, D. Sciti

Oxidation behaviour of a continuous carbon fibre reinforced ZrB₂-SiC composite

Corros. Sci., 123 (2017), pp. 129-138, [10.1016/j.corsci.2017.04.012](https://doi.org/10.1016/j.corsci.2017.04.012)

[Article](#)  [Download PDF](#) [View Record in Scopus](#) [Google Scholar](#)

[14] A. Paul, S. Venugopal, J.G.P. Binner, B. Vaidhyanathan, A.C.J. Heaton, P.M. Brown

UHTC-carbon fibre composites: preparation, oxyacetylene torch testing and characterisation

J. Eur. Ceram. Soc., 33 (2013), pp. 423-432, [10.1016/j.jeurceramsoc.2012.08.018](https://doi.org/10.1016/j.jeurceramsoc.2012.08.018)

[Article](#)  [Download PDF](#) [View Record in Scopus](#) [Google Scholar](#)

- [15] L. Liu, H. Li, W. Feng, X. Shi, K. Li, L. Guo
Ablation in different heat fluxes of C/C composites modified by ZrB₂-ZrC and ZrB₂-ZrC-SiC particles
Corros. Sci., 74 (2013), pp. 159-167, [10.1016/j.corsci.2013.04.038](https://doi.org/10.1016/j.corsci.2013.04.038)
[Article](#)  [Download PDF](#) [View Record in Scopus](#) [Google Scholar](#)
- [16] E.L. Corral, R.E. Loehman
Ultra-high-temperature ceramic coatings for oxidation protection of carbon-carbon composites
J. Am. Ceram. Soc., 91 (2008), pp. 1495-1502, [10.1111/j.1551-2916.2008.02331.x](https://doi.org/10.1111/j.1551-2916.2008.02331.x)
[CrossRef](#) [View Record in Scopus](#) [Google Scholar](#)
- [17] O. Haibo, L. Cuiyan, H. Jianfeng, C. Liyun, F. Jie, L. Jing, X. Zhanwei
Self-healing ZrB₂-SiO₂ oxidation resistance coating for SiC coated carbon/carbon composites
Corros. Sci., 110 (2016), pp. 265-272, [10.1016/j.corsci.2016.04.040](https://doi.org/10.1016/j.corsci.2016.04.040)
[Article](#)  [Download PDF](#) [View Record in Scopus](#) [Google Scholar](#)
- [18] H. Li, L. Zhang, L. Cheng, Y. Wang
Ablation resistance of different coating structures for C/ZrB₂-SiC composites under oxyacetylene torch flame
Int. J. Antimicrob. Agents, 6 (2009), pp. 145-150, [10.1111/j.1744-7402.2008.02320.x](https://doi.org/10.1111/j.1744-7402.2008.02320.x)
[CrossRef](#) [View Record in Scopus](#) [Google Scholar](#)
- [19] R.J. Kerans
The role of coating compliance and fiber/matrix interfacial topography on debonding in ceramic composites
Scr. Metall. Mater., 32 (1995), pp. 505-509, [10.1016/0956-716X\(95\)90828-8](https://doi.org/10.1016/0956-716X(95)90828-8)
[Article](#)  [Download PDF](#) [View Record in Scopus](#) [Google Scholar](#)
- [20] A. Rezaie, W.G. Fahrenholtz, G.E. Hilmas
The effect of a graphite addition on oxidation of ZrB₂-SiC in air at 1500°C
J. Eur. Ceram. Soc., 33 (2013), pp. 413-421, [10.1016/j.jeurceramsoc.2012.09.016](https://doi.org/10.1016/j.jeurceramsoc.2012.09.016)
[Article](#)  [Download PDF](#) [View Record in Scopus](#) [Google Scholar](#)
- [21] F. Yang, X. Zhang, J. Han, S. Du
Processing and mechanical properties of short carbon fibers toughened zirconium diboride-based ceramics
Mater. Des., 29 (2008), pp. 1817-1820, [10.1016/j.matdes.2008.03.011](https://doi.org/10.1016/j.matdes.2008.03.011)
[Article](#)  [Download PDF](#) [View Record in Scopus](#) [Google Scholar](#)
- [22] F. Yang, X. Zhang, J. Han, S. Du
Characterization of hot-pressed short carbon fiber reinforced ZrB₂-SiC ultra-high temperature ceramic composites
J. Alloys Compd., 472 (2009), pp. 395-399, [10.1016/j.jallcom.2008.04.092](https://doi.org/10.1016/j.jallcom.2008.04.092)
[Article](#)  [Download PDF](#) [View Record in Scopus](#) [Google Scholar](#)
- [23] W. Hong, K. Gui, P. Hu, X. Zhang, S. Dong
Preparation and characterization of high-performance ZrB₂-SiC-Cf composites sintered at 1450°C

J. Adv. Ceram., 6 (2017), pp. 110-119, [10.1007/s40145-017-0223-7](https://doi.org/10.1007/s40145-017-0223-7)

[CrossRef](#) [View Record in Scopus](#) [Google Scholar](#)

[24] L. Zoli, D. Sciti

Efficacy of a ZrB₂-SiC matrix in protecting C fibres from oxidation in novel UHTCMC materials

Mater. Des., 113 (2017), pp. 207-213, [10.1016/j.matdes.2016.09.104](https://doi.org/10.1016/j.matdes.2016.09.104)

[Article](#)  [Download PDF](#) [View Record in Scopus](#) [Google Scholar](#)

[25] D. Sciti, A. Natali Murri, V. Medri, L. Zoli

Continuous C fibre composites with a porous ZrB₂Matrix

Mater. Des., 85 (2015), pp. 127-134, [10.1016/j.matdes.2015.06.136](https://doi.org/10.1016/j.matdes.2015.06.136)

[Article](#)  [Download PDF](#) [View Record in Scopus](#) [Google Scholar](#)

[26] A. Vinci, L. Zoli, D. Sciti, C. Melandri, S. Guicciardi

Understanding the mechanical properties of novel {UHTCMCs} through random forest and regression tree analysis

Mater. Des. (2018), [10.1016/j.matdes.2018.02.061](https://doi.org/10.1016/j.matdes.2018.02.061)

[Google Scholar](#)

[27] J. Han, P. Hu, X. Zhang, S. Meng

Oxidation behavior of zirconium diboride-silicon carbide at 1800 °C

Scr. Mater., 57 (2007), pp. 825-828, [10.1016/j.scriptamat.2007.07.009](https://doi.org/10.1016/j.scriptamat.2007.07.009)

[Article](#)  [Download PDF](#) [View Record in Scopus](#) [Google Scholar](#)

[28] S.N. Karlsdottir, J.W. Halloran

Oxidation of ZrB₂-SiC: influence of SiC content on solid and liquid oxide phase formation

J. Am. Ceram. Soc., 92 (2009), pp. 481-486, [10.1111/j.1551-2916.2008.02874.x](https://doi.org/10.1111/j.1551-2916.2008.02874.x)

[CrossRef](#) [View Record in Scopus](#) [Google Scholar](#)

[29] P.A. Williams, R. Sakidja, J.H. Perepezko, P. Ritt

Oxidation of ZrB₂-SiC ultra-high temperature composites over a wide range of SiC content

J. Eur. Ceram. Soc., 32 (2012), pp. 3875-3883, [10.1016/j.jeurceramsoc.2012.05.021](https://doi.org/10.1016/j.jeurceramsoc.2012.05.021)

[Article](#)  [Download PDF](#) [View Record in Scopus](#) [Google Scholar](#)

[30] H. Wu, W. Zhang

Fabrication and properties of ZrB₂-SiC-BN machinable ceramics

J. Eur. Ceram. Soc., 30 (2010), pp. 1035-1042, [10.1016/j.jeurceramsoc.2009.09.022](https://doi.org/10.1016/j.jeurceramsoc.2009.09.022)

[Article](#)  [Download PDF](#) [View Record in Scopus](#) [Google Scholar](#)

[31] J. Han, P. Hu, X. Zhang, S. Meng, W. Han

Oxidation-resistant ZrB₂-SiC composites at 2200 °C

Compos. Sci. Technol., 68 (2008), pp. 799-806, [10.1016/j.compscitech.2007.08.017](https://doi.org/10.1016/j.compscitech.2007.08.017)

[Article](#)  [Download PDF](#) [View Record in Scopus](#) [Google Scholar](#)

- [32] S.S. Hwang, A.L. Vasiliev, N.P. Padture
Improved processing and oxidation-resistance of ZrB₂ ultra-high temperature ceramics containing SiC nanodispersoids
Mater. Sci. Eng. A, 464 (2007), pp. 216-224, [10.1016/j.msea.2007.03.002](https://doi.org/10.1016/j.msea.2007.03.002)
[Article](#)  [Download PDF](#) [CrossRef](#) [View Record in Scopus](#) [Google Scholar](#)
- [33] M. Khoeini, A. Nemati, M. Zakeri, M. Tamizifar, H. Samadi
Comprehensive study on the effect of SiC and carbon additives on the pressureless sintering and microstructural and mechanical characteristics of new ultra-high temperature ZrB₂ ceramics
Ceram. Int., 41 (2015), pp. 11456-11463, [10.1016/j.ceramint.2015.05.110](https://doi.org/10.1016/j.ceramint.2015.05.110)
[Article](#)  [Download PDF](#) [View Record in Scopus](#) [Google Scholar](#)
- [34] J. Watts, G. Hilmas, W.G. Fahrenholtz
Mechanical characterization of ZrB₂-SiC composites with varying SiC particle sizes
J. Am. Ceram. Soc., 94 (2011), pp. 4410-4418, [10.1111/j.1551-2916.2011.04885.x](https://doi.org/10.1111/j.1551-2916.2011.04885.x)
[CrossRef](#) [View Record in Scopus](#) [Google Scholar](#)
- [35] L. Silvestroni, D. Dalle Fabbriche, C. Melandri, D. Sciti
Relationships between carbon fiber type and interfacial domain in ZrB₂-based ceramics
J. Eur. Ceram. Soc., 36 (2016), pp. 17-24, [10.1016/j.jeurceramsoc.2015.09.026](https://doi.org/10.1016/j.jeurceramsoc.2015.09.026)
[Article](#)  [Download PDF](#) [View Record in Scopus](#) [Google Scholar](#)
- [36] D. Gao, Y. Zhang, J. Fu, C. Xu, Y. Song, X. Shi
Oxidation of zirconium diboride-silicon carbide ceramics under an oxygen partial pressure of 200Pa: formation of zircon
Corros. Sci., 52 (2010), pp. 3297-3303, [10.1016/j.corsci.2010.06.004](https://doi.org/10.1016/j.corsci.2010.06.004)
[Article](#)  [Download PDF](#) [View Record in Scopus](#) [Google Scholar](#)
- [37] W.G. Fahrenholtz
Thermodynamic analysis of ZrB₂-SiC oxidation: formation of a SiC-depleted region
J. Am. Ceram. Soc., 90 (2007), pp. 143-148, [10.1111/j.1551-2916.2006.01329.x](https://doi.org/10.1111/j.1551-2916.2006.01329.x)
[CrossRef](#) [View Record in Scopus](#) [Google Scholar](#)
- [38] S.N. Karlsdottir, J.W. Halloran
Formation of oxide films on ZrB₂-15 vol% SiC composites during oxidation: evolution with time and temperature
J. Am. Ceram. Soc., 92 (2009), pp. 1328-1332, [10.1111/j.1551-2916.2009.03052.x](https://doi.org/10.1111/j.1551-2916.2009.03052.x)
[CrossRef](#) [View Record in Scopus](#) [Google Scholar](#)
- [39] A. Vinci, L. Zoli, E. Landi, D. Sciti
Oxidation behaviour of a continuous carbon fibre reinforced ZrB₂-SiC composite
Corros. Sci., 123 (2017), [10.1016/j.corsci.2017.04.012](https://doi.org/10.1016/j.corsci.2017.04.012)
[Google Scholar](#)
- [40] D. Glass
Ceramic matrix composite (CMC) thermal protection systems (TPS) and Hot structures for hypersonic vehicles

15th AIAA Int. Sp. Planes Hypersonic Syst. Technol. Conf. (2008), pp. 1-36, [10.2514/6.2008-2682](#)

[View Record in Scopus](#) [Google Scholar](#)